Electroless deposition of Ni-P composite coatings containing kaolin nanoparticles

K. N. Srinivasan* and PR. Thangavelu

The ability to codeposit particulate matter in a matrix of electroless nickel has led to a new generation of composite coatings with unique properties, such as high hardness wear, abrasion, corrosion and high temperature oxidation resistance. In this paper, the authors report on the development of electroless Ni–P–kaolin composite coating, and the characteristic properties of the selected deposits were evaluated by scanning electron microscopy, energy dispersive X-ray and X-ray diffraction techniques. A good rate of deposition of 12 μm h^{-1} was observed for the optimised concentration of 6 g L^{-1} of kaolin in the bath. For the optimised bath composition and operating conditions, the composite deposit was found to contain 81·7%Ni, 9·8%P and 10·5%kaolin. Heat treatment at 400°C for 1 h results in an increase in the hardness and wear resistance of the composite coating. The corrosion resistance is also highly enhanced by the incorporation of kaolin in the nickel–phosphorus matrix. The crystallite size of the composite coating is 20 nm, and the codeposition of kaolin follows the Langmuir adsorption isotherm.

Keywords: Electroless deposition, Composite coating, Chemical deposition, Nickel–phosphorus–kaolin, Nanocoating, Heat treatment

Introduction

Surface properties such as hardness, wear resistance and corrosion resistance can be improved using various methods, e.g. electroplating, electroless plating, physical vapour deposition, etc. Electroless plating is defined as the autocatalytic deposition of metal ions such as nickel and copper in the presence of reducing agents such as hypophosphite, borohydride, amino borane, etc. Electroless nickel (EN) plating is utilised by the aerospace, automotive, chemical and electrical industries mainly due to its uniformity of deposition over complex geometries, excellent solderability, lubricity, high hardness and high wear and abrasion resistances. Codeposition of various second phase particles leads to the formation of electroless composite coatings. The incorporation of finely sized particles within Ni–P autocatalytic coatings has been found to greatly enhance the mechanical properties (hardness and wear resistance) and corrosion resistance relative to pure metal. In some cases, embedding particles in electroless deposited metals added entirely new features to the performance of the coatings, which increased their use in different industries with applications such as tips for earth moving equipment, moulds, cutting tools and engine parts. Commercially, a number of systems have been described for producing electroless deposited composites. They represent a range of coatings based on dispersed particles of oxides of silicon,[1–12] aluminium[13–33] and zirconium,[34,35] nitrides of boron[36–38] and silicon[39,40] and carbides of tungsten,[41–43] chromium,[44] boron,[45,46] PTFE,[44–50] MoS_2,[51,52] diamond,[53–55] titania,[56–59] etc. Such coatings provide resistance to wear, erosion, corrosion, lubrication, oxidation and fretting, particularly at high temperatures. Light emitting composite EN coatings[60] are a recent and exciting development in the field. These coatings have all the inherent benefits of EN, but when viewed under UV light, they emit a distinct light that can be valuable in authenticating original equipment manufacturer parts in the aircraft industry. Around 335°C phase transformation occurred for both plain Ni–P and composite coatings. By scanning through the available literature on composite coatings, little information seems to be available on high phosphorus EN composite coatings containing submicrometre kaolin particles. Given the benefits afforded by a second phase present in a nickel–phosphorus matrix noted above, systematic studies have been carried out by the authors to prepare Ni–P–kaolin composite coatings by electroless deposition. Plain Ni–P coatings were also prepared for comparison. Deposits were characterised for their structure, morphology, phase transformation behaviour and microhardness at heat treatment temperatures. Grain size has also been calculated for the as deposited and heat treated coatings at crystallisation temperatures. This study examines the effect of deposition time, pH and temperature on the rate of deposition in nickel composite bath. The effect of kaolin content on hardness, wear resistance and corrosion resistance has also been investigated. Structural investigations were carried out using SEM and X-ray diffraction. The improvement in surface properties offered by such composite coatings will have a significant impact on numerous industrial applications,

Central Electrochemical Research Institute (CSIR), Karaikudi, Tamil Nadu 630006, India

*Corresponding author, email knsrinivasan@cecri.res.in

Published by Maney on behalf of the Institute
Received 27 July 2011; accepted 15 September 2011
DOI 10.1179/0020296712Z.0000000009

and in the future, they are likely to secure a more prominent place in the surface engineering of metals and alloys.

Experimental

Electrode preparation

Copper, mild steel and stainless steel electrodes of size 5×5 cm were used. The electrodes were mechanically polished, and the polished specimens were degreased using trichloroethylene. Mild steel panels were used for corrosion studies. Copper panels and stainless steel panels, cut to size where necessary, were used for rate measurement and phosphorus content analysis respectively.

Bath used

The following bath reported elsewhere[61] was used for the studies:

(i) nickel sulphate: 25 g L^{-1}
(ii) sodium citrate: 50 g L^{-1}
(iii) sodium hypophosphite: 20 g L^{-1}
(iv) ammonia to adjust pH: 4–10
(v) kaolin: 1–8 g L^{-1}.

Bath preparation and purification

The required amounts of chemicals were weighed and dissolved in distilled water (3/4 of the total volume required), and then the solution was filtered through a G.4 crucible and made up to the required volume using distilled water. The pH of the solution was adjusted electrometrically by a pH meter (Elico Pvt. Ltd, Hyderabad) using ammonia. The submicrometre kaolin particles used for the study were 99·9% pure, spherical in nature. Kaolinite is a clay mineral, part of the group of industrial minerals, with the chemical composition $Al_2Si_2O_5(OH)_4$. It is a layered silicate mineral with one tetrahedral sheet linked through oxygen atoms to one octahedral sheet of alumina octahedra. Rocks that are rich in kaolinite are known as china clay, white clay or kaolin. The required amount of kaolin powder was cleaned with trichloroethylene washed with water, then treated with 5% sulphuric acid and washed well with water and finally with DI water.

Bath maintenance and control

The temperature of the bath was maintained to within $\pm 2^{\circ}C$ using constant temperature equipment, and the pH of the solution was continuously monitored using a digital pH meter and by appropriate additions of sulphuric acid or ammonia. Bath ingredients nickel sulphate and sodium hypophosphite were analysed regularly and replenished when required. After proper pretreatment, test panels to be EN plated were simply immersed in the bath at the operating temperature. Mechanical agitation at a constant speed of 300 rev min^{-1} was used to achieve uniform suspension of particles in the solution and to prevent agglomeration of the particles. In order to avoid the decomposition of the bath during operation, 2 ppm lead nitrate was added to the bath as a stabiliser.

Effect of bath variables on rate of deposition

Effect of temperature on rate of deposition

Copper panels were mechanically polished, degreased with trichloroethylene, washed, dried and weighed. These copper panels were activated in palladium chloride solution and placed in a 250 mL beaker containing the electroless bath solution (pH 6) with 6 g L^{-1} kaolin particles at different temperatures (40, 50, 60, 70, 80 and 90°C) for 30 min. These panels were then removed, washed, dried and weighed. From the difference in weight, the nickel deposited was calculated. From the weight of nickel deposited, area of copper panel and density of the deposit, the rate of deposition was calculated. Here, it was assumed that the mass contribution of kaolin to the total is negligible given the lower density and the low fraction in the deposit compared to Ni–P

$$\text{Rate of deposition } (\mu\text{m h}^{-1}) = \frac{\text{Weight of Ni deposit (g)} \times 10^4}{\text{Area of panel (cm}^2) \times \text{density of nickel}}$$

Effect of time and pH on rate of deposition

The effect of plating time on the rate of deposition was studied at constant pH of 6 and bath temperature of 90°C. The plating time was varied from 10 to 90 min. Activated copper panels were placed in the electroless bath containing 6 g L^{-1} kaolin at pH values of 4, 4·5, 5, 6, 7, 8 and 10 at 90°C for 30 min. Then, these panels were removed, washed, dried and weighed. From the weight of the deposit, the rate of deposition was calculated, as above.

Microhardness measurements

In general, electroless codeposition processes of second phase particles take place at low temperature, and the chemical interaction between the particles and the matrix is not favoured. The particles are only physically entrapped in the Ni–P matrix. Thus, heat treatment of these coatings is necessary in order to promote phase transitions that will enhance their properties. Hence, the EN coated specimens were heat treated at 400°C. Hardness measurements for all the as plated specimens and the heat treated samples were made on 35 μm thickness deposits using a Vickers's hardness tester with a load of 50 g.

Abrasion resistance measurements

The abrasion resistances of the specimens were measured using Taber Abraser (model AB-5130; Paul n. Gardner Company, Inc.) in both as plated and heat treated conditions. For this test, specimens of size 10×10 cm were used. The abrading wheels were allowed to rotate on the coatings of 35 μm thickness at a load of 1 kg. Before the start of the experiment, the specimens were accurately weighed. Then, the wheels were allowed to rotate against the deposit for 1000 cycles with the above load. After that, the specimens were removed and weighed again. The experiment was repeated for another 1000 cycles. The average weight loss was taken as the Taber wear index or abrasion resistance

Taber wear index = Weight loss (mg) for 1000 cycles

X-ray diffraction measurements

X-ray diffraction patterns (Make-Analytical, USA Instruments) for the electroless deposited composite nickel specimens were made in both as plated and heat

treated (400°C) conditions to determine the amorphous or crystalline nature of the deposits.

Scanning electron microscopic studies

The morphology of the electroless deposits with and without kaolin was examined under high magnification ($\times 1000$) to assess the grain size, deposit nature, heterogeneities and pores present in the deposits using a scanning electron microscope (model S-3000H; Hitachi). The scanning electron microscope, which makes use of reflected primary electrons and secondary electrons, enables one to obtain information from regions that cannot be examined by others. The EN plated specimens were cut into 1×1 cm size, mounted suitably and examined under the microscope. Nickel, phosphorus and kaolin contents present in the coating were evaluated using energy dispersive X-ray (EDX) studies.

Impedance measurements

The ac impedance spectrum was obtained for the EN deposits with and without kaolin. Impedance measurements were carried out using a three-electrode cell assembly (IM6 Electrochemical Impedance Analyser). A frequency range of 100 kHz to 10 mHz was impressed on the system. In this experiment, the ac voltage is superimposed on the rest potential on an electroless deposited electrode immersed in 5%NaCl. Using the Nyquist plot, the charge transfer resistance and double layer capacitance values were calculated.

Results and discussion

Effect of temperature on rate of deposition

Table 1 shows the influence of temperature on the rate of deposition in the presence of 6 g L^{-1} kaolin. From the table, we infer that the rate of deposition increases with an increase in temperature. When the temperature is >90°C, the bath decomposed, resulting in the formation of a powdery deposit. Hence, 90°C was fixed as the operating temperature for carrying out further studies.

Table 1 Effect of temperature on rate of deposition from bath (pH of 6·0) with 6 g L^{-1} of kaolin

Sample no.	Temperature/°C	Rate of deposit/μm h^{-1}
1	50	2·3
2	60	2·9
3	70	6·2
4	80	8·0
5	90	12·3

Table 2 Effect of time on rate of deposition from bath (temperature of 90°C; pH 6) with 6 g L^{-1} of kaolin

Sample no.	Deposition time/min	Deposit thickness/μm	Deposition rate/μm h^{-1}
1	10	5·3	31·8
2	15	6·9	27·6
3	20	7·7	23·1
4	25	8·4	20·2
5	30	8·8	17·6
6	45	9·3	12·4
7	60	9·8	9·8
8	90	12·3	8·2

Effect plating time on rate of deposition

Table 2 shows the variation in rate of deposition with time in the basic electroless bath. It shows that a very high rate was observed initially, and this reduces with deposition time. This may be due to the ready deposition of EN on freshly activated mild steel surface. With time, reduction in the deposition rate takes place as the surface becomes covered with freshly deposited nickel surface.

Effect of pH on rate of deposition

Table 3 shows the change in rate of deposition with pH. The pH of the solution was varied from 4 to 8 while keeping other parameters constant. It is seen from the table that increasing the bath pH increases the rate of deposition and has a considerable effect on the rate of deposition. In electroless deposition of nickel with hypophosphite reducer, two simultaneous reactions, i.e. reduction and oxidation processes, are taking place on the catalytic surface. In the reduction processes, two competing reactions nickel ion and hydrogen ion reduction are taking place. Reduction of nickel ion occurs through electrons produced in the process of interaction of hypophosphite with water

$$H_2PO_2^- + H_2O \rightarrow H_2PO_3^- + 2H^+ + 2e$$

$$Ni^{2+} + 2e \rightarrow Ni^0$$

$$2H^+ + 2e \rightarrow H_2$$

With the increase in acidity of the solution, the probability of interaction of protons with electrons is increased, leading to the reduction of the coefficient of utilisation of hypophosphite together with reduction of nickel ions. Thus, the rate of hydrogen evolution becomes favoured over nickel ion reduction in high hydrogen ion concentration (low pH). Hydrogen ion present in the electrolyte favours the phosphorus formation

$$H_2PO_2^- + e \rightarrow P + 2OH^-$$

Effect of kaolin on hardness of deposits

Table 4 shows the effect of the presence of kaolin on the hardness of Ni–P coatings with and without heat treatment. It is observed from the table that the hardness is increased as the kaolin content in the bath is increased due to the incorporation of more hard kaolin particles in the deposit. After heat treatment at 400°C, the kaolin

Table 3 Effect of pH on rate of deposition (bath temperature 90°C) with 6 g L^{-1} of kaolin in bath

Sample no.	pH	Rate of deposition/μm h^{-1}
1	4	6·0
2	4·5	6·9
3	5·0	7·6
4	6·0	12·3
5	7·0	15·7
6	8·0	18·3

particles may get sintered, leaving larger kaolin films on the surface of the deposit accounting for the higher hardness of this composite coating.

Effect of kaolin on wear resistance of deposits

Table 5 gives the values of wear resistance taken by Taber Abraser at a load of 1 kg for 1000 cycles on the plated as well as heat treated deposits. It is seen from the table that the wear resistance is greater for the coatings containing kaolin particles than with Ni–P alloy in both as plated and heat treated conditions. Heat treatment enhances the wear resistance of the composite coatings. It is to be also noted from Table 6 that as the concentration of kaolin in the bath increases, its content in the deposit also increases at the cost of nickel and phosphorus up to 6 g L^{-1} and thereafter appears to attain a steady state, remaining at a constant deposited level.

Surface topography

Figures 1 and 2 show the SEM photographs of the Ni–P coatings with and without kaolin present in the matrix in the as deposited conditions. It seems evident from the figures that there is a uniform dispersion of kaolin particles in the deposit. Figure 3 shows the cross-sectional view of the composite coating. It is seen from this that there is a uniform distribution of particles in the Ni–P matrix. X-ray diffraction measurements (Figs. 4 and 5) also confirm the presence of kaolin particles in the Ni–P matrix. It is seen from these scans that the peaks obtained for nickel–phosphorus with and without kaolin are amorphous in nature, and the crystallite size calculated using the Scherrer equation is shown to be 25 and 20 nm respectively. The EDX spectrum of the composite coating

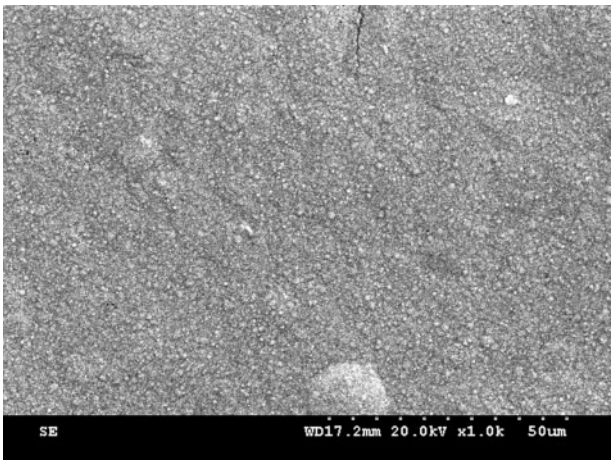

1 Image (SEM) of Ni–P

(Fig. 6) obtained from the bath containing 6 g L^{-1} of kaolin confirms the presence of kaolin particles in the composite coating.

Effect of kaolin on corrosion resistance of deposits

Table 7 shows the corrosion resistance of the composite coating with and without heat treatment. Figures 7 and 8 show the impedance spectra obtained for the composite coating with and without heat treatment. Using Nyquist plots, the charge transfer resistance values of the above reaction are calculated as the x intercept of the semicircle, where the x axis represents the real part of the impedance. Perfect semicircles are encountered in the case where the electrochemical reaction of interest is under charge transfer control. Where the reactions are partially under charge transfer and mass transport control, there is a drag noted in the semicircular plot. When the reaction is under diffusion control, a rising portion is noted in the low frequency end of the plot. In addition, any looping at the tail end of the plot is attributed to the contribution of the Warburg impedance.

In most of the impedance plots, the semicircles are not complete, particularly at the low frequency end, and they need to be estimated by extrapolation of a best fitted half circle for the experimental values. The

Table 4 Effect of concentration of kaolin particles in bath on hardness of coating

Sample no.	Concentration of kaolin in the bath/g L^{-1}	Vickers hardness (load 50 g)	
		as plated	heat treated
1	0	550	799
2	1	567	820
3	4	600	930
4	6	650	990
5	8	656	996

Table 5 Effect of concentration of kaolin particles in bath on wear resistance of coating (load 1 kg)

Sample no.	Kaolin/g L^{-1}	Wear (as plated)/mg (1000 cycles)	Wear (after heat treatment)/mg (1000 cycles)
1	0	0·0259	0·0212
2	1	0·0232	0·0200
3	4	0·0221	0·0123
4	6	0·0212	0·0120
5	8	0·0182	0·0150

Table 6 Effect of concentration of kaolin particles in bath on weight percentage of Ni, P and kaolin in deposit

Sample no.	Concentration of kaolin in the bath/g L^{-1}	Composition of the deposit/wt-%		
		Ni	P	Kaolin
1	0	89·32	11·60	…
2	1	82·50	10·16	7·45
3	4	80·48	10·90	8·62
4	6	81·71	9·82	10·47
5	8	79·62	9·36	11·02

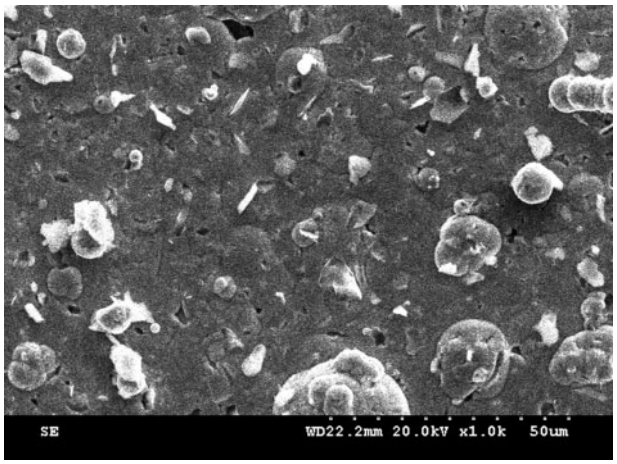

2 Image (SEM) of Ni–P–kaolin

corrosion resistance of the deposits with kaolin is higher in both as plated and heat treated conditions than without kaolin content. The high corrosion resistance of the deposit may be due to the hard nature of the kaolin particles and their uniform distribution in the Ni–P matrix, as evidenced from the cross-sectional study of the composite coatings.

Mechanism of incorporation of kaolin in nickel–phosphorus matrix

The incorporation of kaolin particles seems to be mainly due to mechanical effects and little due to the electrophoretic effects of the hydrophobic particles. As the particles strike the surface, they are included in the nickel alloy being deposited and become a part of the cermet. There is no molecular bond between the particles and the metal matrix.[62,63] The codeposition of particles is governed by a two-step adsorption mechanism. In the first step, the dispersed particles in the bath are transported to the surface of the electrode by mechanical action and are physically adsorbed due to the fluidal action. In the second step, these physically adsorbed particles dehydrate because

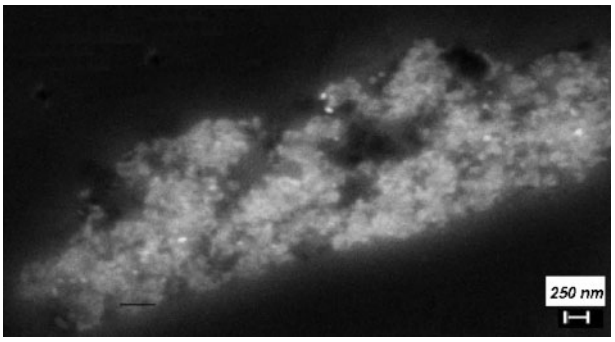

3 Cross-sectional view of Ni–P–kaolin composite

of the strong electric field of the Helmholtz layer at the electrode, and a strong irreversible chemical adsorption of the particles on the electrode takes place. The adsorbed particles are embedded by reduced metal or alloys. The physical adsorption is Langmuir adsorption.[64] Langmuir adsorption studies have been carried out and assessed in the present study. The values of fractional surface coverage θ were obtained using values of rates of deposition in the presence and absence of kaolin particles r_o from the weight gain method. The fractional surface coverage is written as

$$\theta = 1 - (r_0/r_t)$$

Suppose that the adsorption of all the kaolin particles on the metal surface follows the Langmuir isotherm, then, the fractional surface coverage is given by

$$\theta = KC_0/1 + KC_0$$

where C_o denotes the bulk concentrations of the additives, and K is the adsorption constant. The above two equations can be combined and rearranged to give

$$(1/r_t) = (1/r_0) + (K/r_0)C_0$$

Table 8 shows the effect of the rate of deposition on the concentration of kaolin particles in the bath. It is seen from the table that there is an increase in the rate of deposition

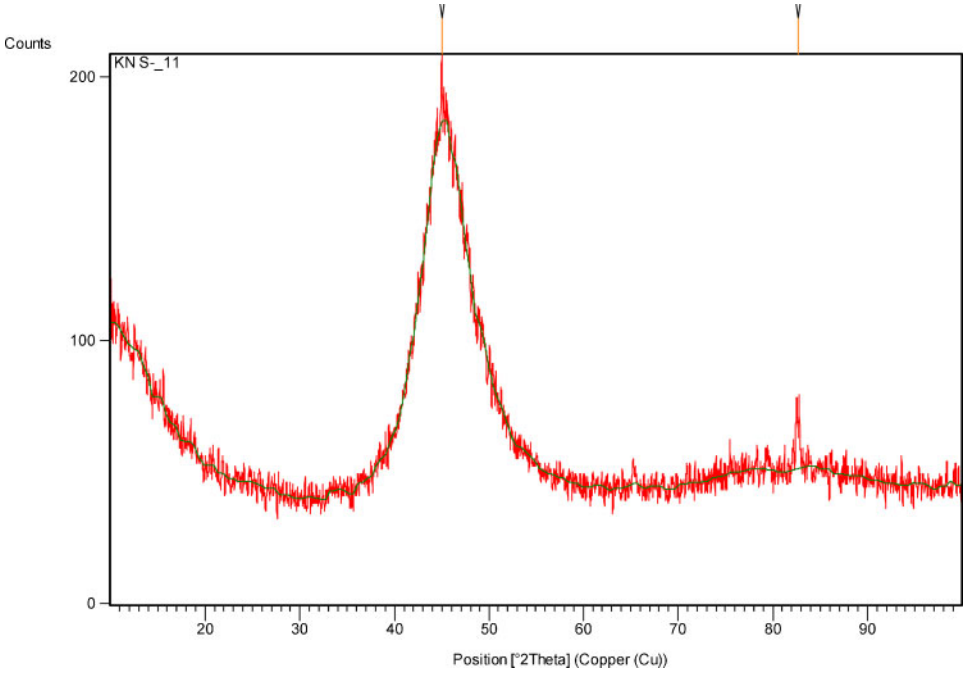

4 X-ray diffraction pattern for Ni–P–kaolin coating as deposited

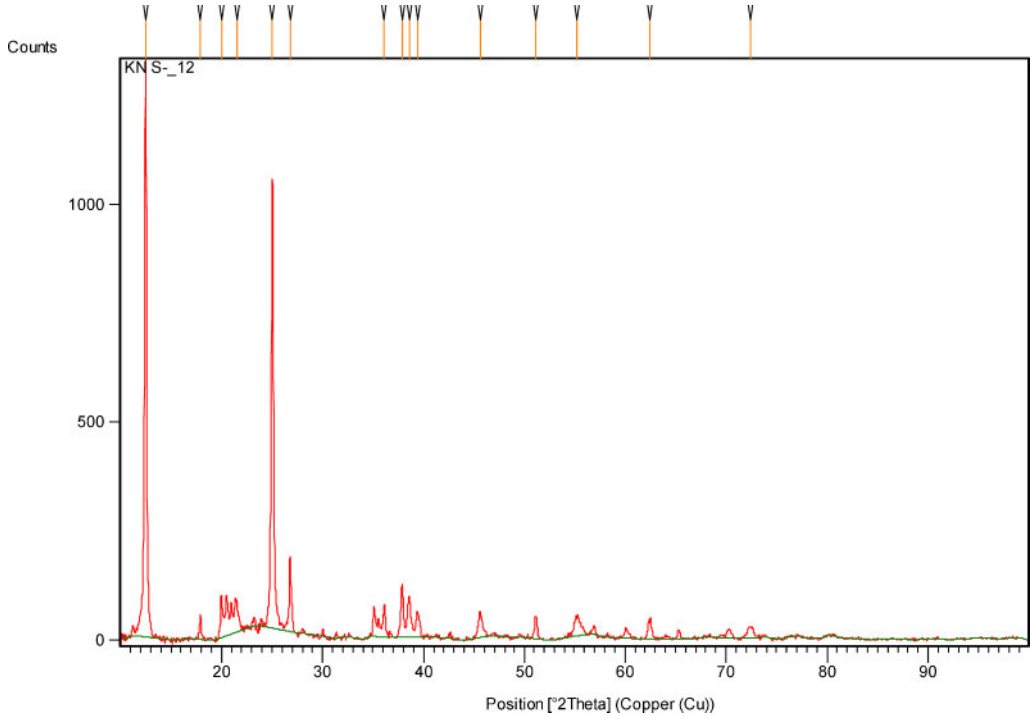

5 X-ray diffraction pattern for Ni–P–kaolin coating after heat treatment

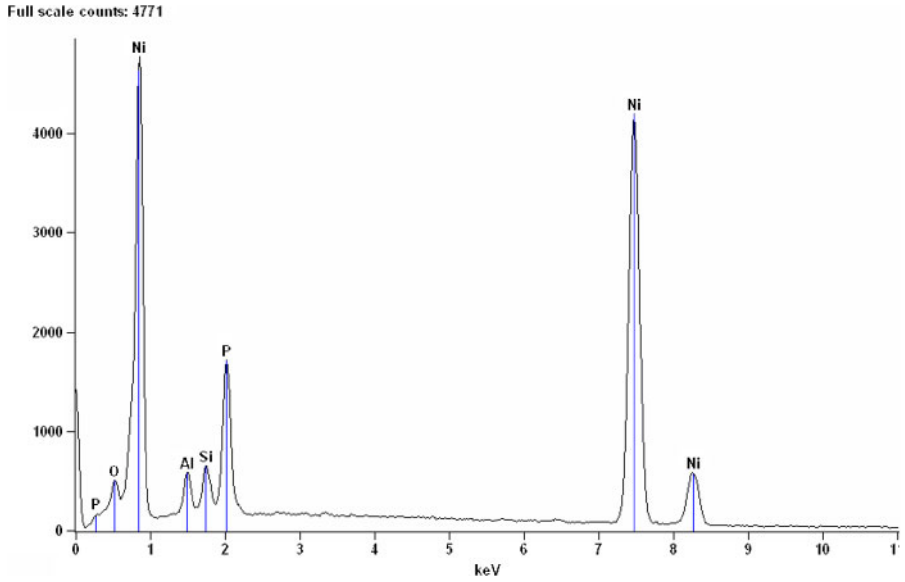

6 Spectrum (EDX) of Ni–P–kaolin (6% in bath)

with concentration of kaolin particles in the bath. The increase in the rate may be due to the higher incorporation of inert particles in the nickel–phosphorus matrix. The Langmuir isotherm was also tested by plotting $1/r_t$ versus C_o, where C_o denotes the bulk concentrations of kaolin, and r_t is the rate of deposition. A straight line relationship was obtained (Fig. 9) in the presence of kaolin, thereby confirming that the adsorption process obeys the Langmuir adsorption isotherm.

The relationship between the rate of reaction and temperature in EN plating can be expressed through the Arrhenius equation

Table 7 Corrosion resistance of composite coating obtained by impedance spectra

Sample no.	Concentration of kaolin in the bath/g L^{-1}	As plated R_{ct}/Ω cm^2	After heat treatment R_{ct}/Ω cm^2
1	0	2·126	5·391
2	6	3·193	8·221

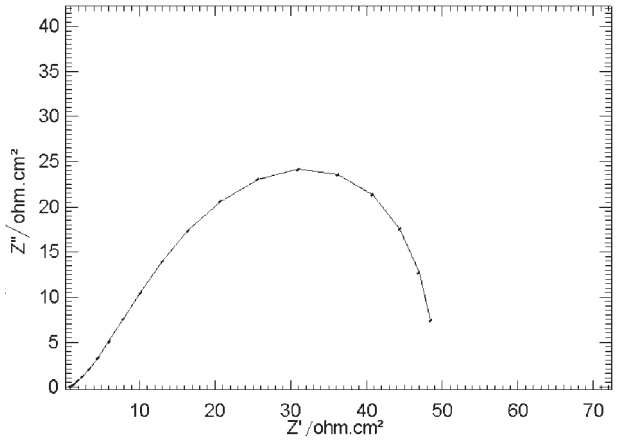

7 Impedance spectra for as plated composite coating

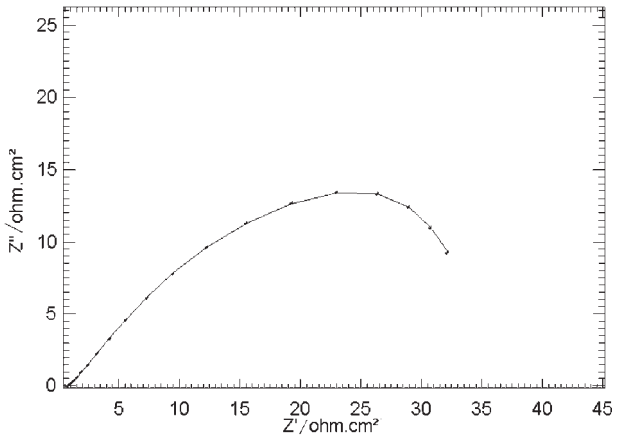

8 Impedance spectra for composite coating after heat treatment

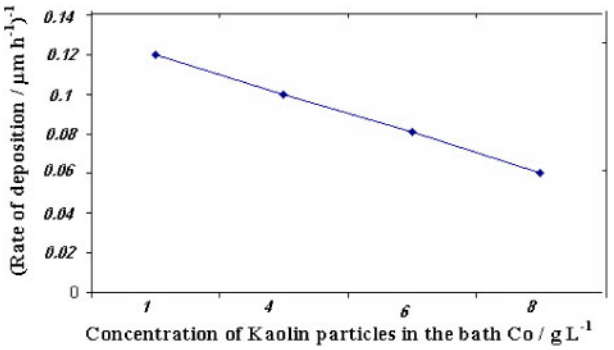

9 Langmuir isotherm plot for EN composite bath in presence of different concentrations of kaolin

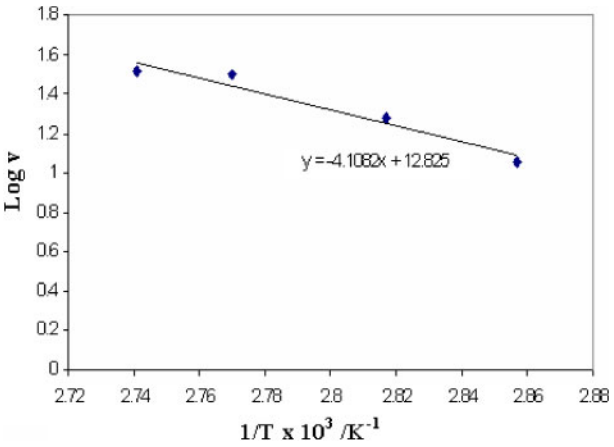

10 log *v* versus 1/*T* curves of EN in absence of kaolin

$$v = Ae^{-E_a/RT}$$

$$\log\ v = \log\ A - E_a/RT$$

From the slope of the log v versus $1/T$ straight line plot, the activation energy E_a can be calculated

$$E_a = \text{Slope} \times 2{\cdot}303 \times R$$

where R is the gas constant. Figures 10 and 11 represent the Arrhenius plots for the EN process in the presence and absence of kaolin at their optimum concentration. The values of E_a calculated from the figures are $-59{\cdot}16$ and $-78{\cdot}66$ kJ mol^{-1} respectively. From the results, it is evident that the presence of kaolin will be able to reduce the activation energy of the EN process when compared to the bath without kaolin. In the present case, the adsorption of the compounds on the metal surface is found to obey the Langmuir adsorption, and this leads to a decrease in activation energy values of the plating process on the metal surface.

Table 8 Effect of concentration of kaolin in bath on rate of deposition (bath temperature 90°C and bath pH 6)

Sample no.	Concentration of kaolin in the bath/g L^{-1}	Rate of deposition/μm h^{-1}
1	1	8·3
2	4	10·0
3	6	12·24
4	8	16

Conclusions

A new bath formulation has been developed for producing nanocomposite coatings of Ni–P–kaolin, and given below is the optimum concentration and operating conditions.

1. Nickel sulphate: 25 g L^{-1}.
2. Sodium citrate: 50 g L^{-1}.
3. Sodium hypophosphite: 20 g L^{-1}.
4. pH (adjust by ammonia): 6·0.
5. Kaolin: 6 g L^{-1}.
6. Lead nitrate: 2 ppm L^{-1}.
7. Temperature: 90°C.

At this concentration, the deposit was found to contain 81·7 wt-%Ni, 9·8 wt-%P and 10·5 wt-% kaolin. Nickel–phosphorus deposits with and without kaolin are amorphous in nature, and the crystallite size calculated using the Scherrer equation is 25 and 20 nm respectively. The codeposition of kaolin follows the Langmuir adsorption isotherm. There is an increase in hardness with the incorporation of kaolin due to the hard nature of the kaolin particles. Wear resistance and corrosion

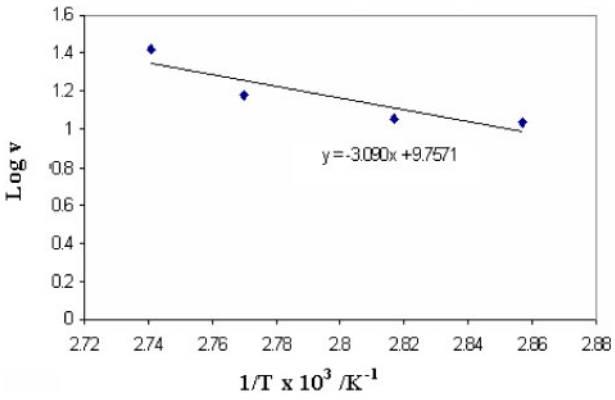

11 log *v* versus 1/*T* curves of EN in presence of kaolin

resistance are very much improved in the presence of kaolin particles after heat treatment. Hence, the coating seems suitable for engineering applications where high wear resistance and hardness are required.

References

1. E. Knaak: *Galvanotechnik*,1991, **82**, 3400.
2. O. Takano, M. Nishira and M. Sugimoto: *J. Met. Finish. Soc*., 1988, **39**, 705.
3. M. Matsuoka, T. Hotta, T. Tamura and T. Hayashi: *J. Surf. Finish. Soc*., 1989, **40**, 831.
4. M. Nishira, M. Sugimoto and O. Takano: *J. Surf. Finish. Soc*., 1990, **41**, 407.
5. Z. C. Guo: *Mater. Protect*.,1992, **25**, 34.
6. Z. C. Guo and W. P. Chen: *Electroplat. Pollut. Control*, 1993, **13**, 70.
7. F. Gammel and P. Filke: *Galvanotechnik*, 1994, **85**, 1139.
8. M. Nishira, K. Yamagishi and M. Sugimoto: *J. Surf. Finish. Soc*., 1991, **42**, 84.
9. H. Xinmin and D. Zongang: *Trans. Inst. Met. Finish*., 1992, **70**, 84.
10. M. R. Kalantary, K. A. Holbrook and P. B. Wells: *Trans. Inst. Met. Finish*., 1993, **71**, 55.
11. X. L. Hong, X. R. Wang and Y. Qian: *Electroplat. Finish. (China)*, 1995, 36.
12. M. Rezrazi, A. Grosjean, J. Takadoum and P. Bercot: *Surf. Coat. Technol.*, 2001, **137**, 92–96.
13. D. Vojtech: *Mater. Manuf. Process.*, 2009, **24**, 754–757.
14. F. Bigdeli and S. R. Allahkaram: *Int. J. Mod. Phys.*, 2008, **22**, (18–19), 3031–3036.
15. M. Sareet, C. Muller and A. Amell: *Surf. Coat. Technol.* 2006, **201**, (1–2), 389–395.
16. Y. T. Wu, L. Lei, B. Shen and W. B. Hu: *Surf. Coat. Technol.*, 2006, **201**, (1–2), 441–445.
17. J. Q. Gao, L. Liu, Y. T. Wu, B. Shen and W. B. Hu: *Surf. Coat. Technol.*, 2006, **200**, (20–21), 5836–5842.
18. B. Mueller and H. Ferkel: *Nanostruct. Mater.*, 1998, **10**, 1285.
19. H. K. Kloos, E. Wagner and E. Broszeit: *Z. Werkstofftech.*, 1980, **11**, (3), 77–82.
20. B. Olberts: *Giesserei*, 1982, **69**, 72.
21. J. Bielinnsky, W. Gluszewski and J. Przylusla: *Galvano-Ref*., 1988, **35**, 107.
22. H. Honma and K. Kanemitsu: *Plat. Surf. Finish*., 1987, **74**, 62.
23. K. L. Lin and P. J. Lai: *Plat. Surf. Finish*., 1989, **76**, 48.
24. M. Pushpavanam: *Bull. Electrochem*., 1992, **8**, 399.
25. L. Wang, Y. Gu and G. Zhang: *Electroplat. Finish. (China)*, 1994, **13**, 9.
26. J. Bielinsky, W. Gluszewski, W. Syokarski and J. Przyluski: *Galvanotechnik*, 1995, **86**, 81.
27. J. Q. Gao, Y. T. Wu, L. Liu and W. B. Hu: *Mater. Lett*., 2005, **59**, (2–3), 391–394.
28. K. N. Shretha, D. B. Hamal and T. Saji: *Surf. Coat. Technol.*, 2004, **183**, (2–3), 247–253.
29. C. F. Jakob Erler and R. Nutsch: Proc. 97th Meet. Electrochemical Society, Toronto, Ont., Canada, *J. of Electroplating & Finishing*, 2000, 1, 329.
30. J. N. Balaraju, D. Kalavathi and K. S. Rajam: *Surf. Coat. Technol.*, 2006, **200**, (12–13), 3933–3941.
31. M. Pushpavanam and B. A. Shenoi: *Met. Finish*., 1977, **75**, (4), 38–43.
32. A. S. Hamdy, M. A. Shoeib, H. Hady and O. F. Abdel Salam: *J. Appl. Electrochem.*, 2008, **38**, 385–394.
33. S. Mirzamohammadi, R. Kiarasi, M. K. Aliov, A. R. Sabur and A. Hansanzedeh-Tabrizi: *Trans. Inst. Met. Finish*., 2010, **88**, (2), 93–99.
34. S. B. Sharma, R. C. Agarwala, V. Agarwala and K. G. Satyanarayana: *J. Mater. Sci*., 2002, **37**, 5247.
35. Y. W. Song, D. Y. Shan and E. H. Han: *Mater. Corros*., 2007, **58**, (7), 506–510.
36. A. Ovidio Leo'n, M. H. Staia and H. E. Hintermann: *Surf. Coat. Technol.*, 1999, **120**, 641–645.
37. M. Pushpavanam and S. R. Natarajan: *Met. Finish*., 1995, **93**, 97.
38. A. Gajewska-Midzialek, B. Szeptycka and A. Nakoniaczny: *Trans. Inst. Met. Finish.*, 2009, **87**, (3), 141–144.
39. C. M. Das, P. K. Limaye, A. K. Grover and A. K. Suri: *J. Alloys Compd*, 2007, **436**, (1–2), 328–334.
40. J. N. Balaraju, V. Selvi, V. Ezhil and K. S. Rajam: *Trans. Inst. Met. Finish.*, 2010, **88**, (6), 311–316.
41. M. Amirjan, K. Zangeneh-Madar and N. Parvin: *Powder Metall.*, 2010, **53**, (3), 218–222.
42. H. J. Chen, L. L. Wang, W. Q. Huang and L. Hao: *Corros. Eng. Sci. Technol.*, 2010, **45**, (3), 235–239.
43. Z. Abdel Hamid, S. A. El Bady and A. Abdel: *Surf. Coat. Technol.*, 2007, **201**, (12), 5948–5953.
44. J. K. Dennis, S. T. Sheikh and E. C. Silverstone: *Trans. Inst. Met. Finish*., 1981, **59**, (4), 118–122.
45. A. Araghi and M. H. Paydar: *Mater. Des.*, 2010, **31**, (6), 3095–3099.
46. E. Ebrahimian-Hosseinabadi, K. Azari-Dorchech and S. M. Moonir Vaghefi: *Wear*, 2006, **260**, (1–2), 123–127.
47. K. N. Srinivasan and S. John: *Surf. Eng*., 2005, **21**, (2), 156–160.
48. S. S. Tulsi: *Trans. Inst. Met. Finish*., 1983, **61**, 147.
49. Z. S. He, L. Wang, Y. Gu and G. Zhang: *Mater. Protect*., 1995, **28**, 16.
50. H. Matsuda, M. Nishira, Y. Kiyono and O. Takano: *Trans. Inst. Met. Finish*., 1995, **73**, 16.
51. A. Grosjean, E. M. Rezrazi and M. Tachez: *Galvano Organo*., 1996, **43**, 66.
52. X. G. Hu, P. Jiang, J. C. Wan, Y. F. Xu and X. J. Sun: *J. Coat. Technol.*, 2009, **6**, (2), 275–281.
53. J. Lukschanded: *Oberflache – Surface*, 1991, **32**, 8.
54. C. C. Hung, C. C. Lin and H. C. Shih: *Diamond Relat. Mater.*, 2008, **17**, (4–5), 853–859.
55. M. Petrova, Z. Noncheva and Ek. Dobreva: *Trans. Inst. Met. Finish*., 2011, **89**, (2), 89–94.
56. S. John, K. N. Srinivasan, P. M. Kavimani, K. Hari Krishnan, J. Praveen and M. Ganesan: *Plat. Surf. Finish*., 2005, **92**, (5), 62–66.
57. J. Novakovic, P. Vassiliou, K. Samara and Th. Argyropoulos: *Surf. Coat. Technol.*, 2006, **201**, (3–4), 859–901.
58. Y. Dai, Q. Li, F. Luo, H. Guo and H. X. Zhu: *Trans. Inst. Met. Finish*., 2011, **89**, (3), 162–168.
59. Q. Li, H. Gao, J. P. Wang and B. Chen: *Trans. Inst. Met. Finish*., 2009, **87**, (3), 149–154.
60. A. Santhi, K. N. Srinivasan and S. John: *Electroplat. Finish. (China)*, 2009, **28**, (1), 15–20.
61. K. N. Srinivasan, S. Karthikeyan, T. Vasudevan and S. John: *Electroplat. Finish.(China)*, 2007, **26**, (1), 1–6.
62. F. N. Hubbell: *Trans. Inst. Met. Finish*., 1978, **56**, 65.
63. F. N. Hubbell: *Plat. Surf. Finish*., 1978, **65**, (12), 58.
64. N. Guglielmi: *J. Electrochem. Soc*., 1972, **119**, (8), 1009–1012.